The Need to Use Generalized Continuum Mechanics to Model 3D Textile Composite Forming

Philippe Boissé, Renzi Bai, Julien Colmars, Nahiene Hamila, Biao Liang, Angela Madeo

The Need to Use Generalized Continuum Mechanics to Model 3D Textile Composite Forming

P. Boisse[1], R. Bai1, J. Colmars[1], N. Hamila[1], B. Liang[1], A. Madeo[2]

Abstract 3D textile composite reinforcements can generally be modelled as continuum media. It is shown that the classical continuum mechanics of Cauchy is insufficient to depict the mechanical behavior of textile materials. A Cauchy macroscopic model is not capable of exhibiting very low transverse shear stiffness, given the possibility of sliding between the fibers and simultaneously taking into account the individual stiffness of each fibre. A first solution is presented which consists in adding a bending stiffness to the tridimensional finite elements. Another solution is to supplement the potential of the hyperelastic model by second gradient terms. Another approach consists in implementing a shell approach specific to the fibrous medium. The developed Ahmad elements are based on the quasi-inextensibility of the fibers and the bending stiffness of each fiber.

Keywords 3D textile reinforcements · Continuum mechanics models · Second gradient models · Finite element curvature

1 Introduction

Most composite structures are laminated, i.e. made of 2D layered reinforcements. These laminated composites have been used successfully for several decades in the aeronautics [1, 2], automotive [3], marine [4] and civil engineering sectors [5, 6]. However, some mechanical properties of these laminated composites are low. In particular, their resistance to delamination cracking due to their low interlaminar fracture toughness are weak points of these materials. Moreover, the use of these laminated composites can lead to manufacturing difficulties. The labour required to drape the plies can be costly when the thickness of a composite part is large. Moreover, the realization of complex shapes often requires to build them from the assembly of several laminated parts. Because

✉ P. Boisse
Philippe.Boisse@insa-lyon.fr

[1] LaMCoS, INSA-Lyon, Université de Lyon, F-69621 Lyon, France

[2] SMS-ID, INSA-Lyon, Université de Lyon, F-69621 Lyon, France

delamination failure is unacceptable in some critical parts, particularly in aeronautics applications, 3D fiber architecture composites have been proposed. Interlocks fabrics are among the most interesting reinforcements on the market [7–15]. The weaving of the warp yarns connects two layers of weft yarns together. Therefore, the weaving links all yarns through the thickness (Fig. 1a). Although there is no actual yarn in the thickness, the material obtained is 3D. The properties through thickness are much improved. In particular, delamination tendencies of laminated composites are avoided. Complex interlock weaves can be obtained thanks to the recent advances in the field of Jacquard weaving [16, 17]. Due to their resistance to delamination, interlock fabrics are used for certain aircraft applications such as aeronautical engine fan blades [18].

When simulating the forming of 3D reinforcements whose thickness is large, the strains and stresses throughout the thickness of the preform must be calculated. Although mesoscopic approaches exist (which model each yarn in contact with its neighbours) [19–22], a textile reinforcement can generally be modelled by a continuous medium. A FE. analysis using 3D elements can be performed in the general case. The three-dimensional finite element simulation of the three-point bending of a textile reinforcement shows, in section 2, that this simulation leads to certain discrepancies with experiment when using a constitutive law within the standard mechanics of the Cauchy continuum. The aim of this paper is to highlight the reasons for these difficulties and to propose solutions for the modeling of the flexion of textile reinforcements in particular interlocks. It will be shown that generalized continuum mechanics approaches [23–27] make it possible to obtain correct 3D solutions for the bending of the textile reinforcements. Another possible approach is to add a bending stiffness to the 3D finite elements in calculating the curvature from the position of the neighbouring elements [28]. Finally, section 5 presents a shell formulation for simulations of the forming of fibrous reinforcements which correctly models their kinematics and the deformation of the points in their thickness [29, 30].

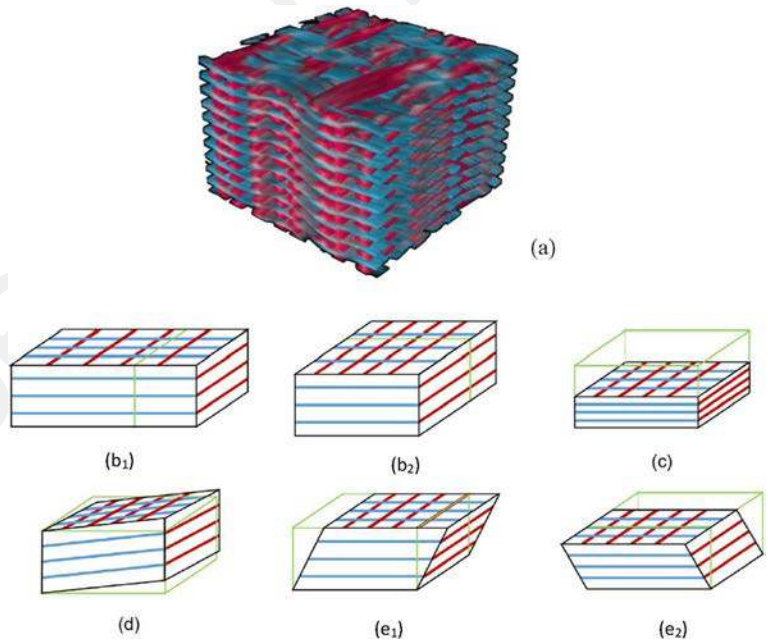

Fig. 1 Deformation modes of a layer to layer interlock reinforcements **a** ply to ply interlock [31], (**b1** and **b2**) stretches, **c** transverse compression, **d** in-plane shear and (**e1** and **e2**) transverse shears

2 Cauchy' Standard Continuum Mechanics Limitations in the Case of Textile Reinforcements

2.1 A Hyperelastic Model (of Cauchy) for Interlock Reinforcements

The deformation of thick reinforcements, in particular the phenomena in the reinforcement thickness can be analysed by three-dimensional finite element modelling. We consider interlock reinforcements which consist of warp and weft yarn directions which are weaved together in thickness (Fig. 1a [31]). Delamination is avoided by this internal constitution. There is no yarn in the thickness direction. The thickness can be important and reach several centimetres for example in the root of a aero-engine fan blade [16, 28, 32]. For this type of interlock reinforcements (with two directions of yarns Fig. 1a), a 3D hyperelastic law has been developed in [33]. This type of material is considered to have six deformation modes (Fig. 1). The extensions in the warp and weft directions are depicted by the invariants I_{elong1} and I_{elong2}. The in plane shear is depicted by the invariant I_{cp}. Transverse compaction is depicted by the invariant I_{comp}. Finally the transverse shears in the warp and weft directions are depicted by the invariants I_{ct1} and I_{ct2}.The deformation energy is assumed to be the sum of deformation energies corresponding to the six deformation modes:

$$w = w_{elong1}\left(I_{elong1}\right) + w_{elong2}\left(I_{elong2}\right) + w_{comp}\left(I_{comp}\right) + w_{cp}\left(I_{cp}\right) + w_{ct1}\left(I_{ct1}\right) + w_{ct2}\left(I_{ct2}\right) \quad (1)$$

The six invariants above can be expressed in terms of the theoretical invariants of an orthotropic elastic material [28, 33, 34]. Tension, transverse compaction, transverse shear and transverse shear experimental tests identify the six potential deformation energies (Eq. 1) in particular in the case of interlock reinforcement Fig. 1a [28, 33]. This hyperelastic model is specific to thick interlocks reinforcements. Such a model is one of Cauchy's standard models.

2.2 Three-Point Bending. Experiments and Simulation

The experimental three-point bending of an interlock reinforcement (thickness = 15 mm) was carried out Fig. 2. The simulation of the bending is performed using the hyperelastic model presented above and 3D height node elements (Fig. 2c). The simulation provides positions after deformation of the normals (material lines initially perpendicular to the mean surface) of the interlock reinforcement which are in fairly good agreement with the experiment. These directions of the normals after deformation are very specific and far from being perpendicular to the deformed mean-surface. This is a specificity of fibrous reinforcements. Nevertheless, the simulation presents some less satisfactory points. The parts of the specimen that are external to the supports have remained almost horizontal (Fig. 2c) as they rise in the experiment. (Fig. 2b).

2.3 Two Simplified Models to Analyse the Difficulties of the Cauchy Hyperelastic Model

A simplified model is presented Fig. 3 with the objective of explaining this difficulty. A system of parallel hinged bars (four-bar system) is considered Fig. 3a. This system has zero transverse shear stiffness which is almost the case for the interlock reinforcement. The tension stiffness of the bars is high and makes them almost inextensible. Although very simplified, this model is close to the behaviour of interlock reinforcement. A vertical displacement imposed at the

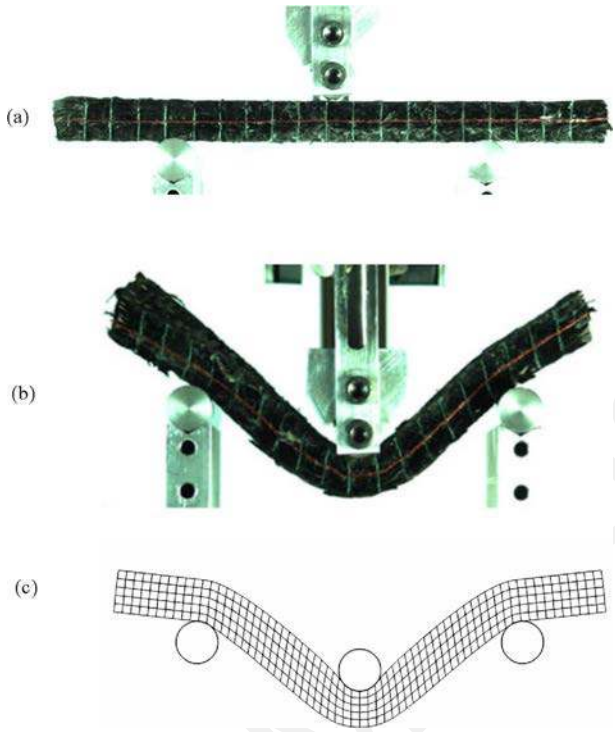

Fig. 2 **a** Initial state of the interlock reinforcement, **b** Experimental three point bending, **c** simulation based on a hyperelastic model of Cauchy

center of the model, leads to a deformation due to transverse shear in the part of the model between the support points (Fig. 3b). The deformed shapes obtained using the hyperelastic continuous model (Fig. 2c) and the simplified model with articulated bars (Fig. 3b) are close. The two parts of the models outside the supports remained almost horizontal. This is due to the very low transverse shear stiffness in both cases. The one of the hinged bar system is effectively nil. The transverse shear stiffness of the interlock reinforcement is very weak due to the possible slippage between the fibres.

An elevation of the ends is obtained (Fig. 3c) when beams replace the bars in the simplified model. The bending stiffness of the fibres in the interlock reinforcement is represented by that of the beams. The number of fibres is large and if each of them has a low bending stiffness given its diameter, the total of fibres, i.e. the interlock reinforcement has a bending stiffness which leads to the elevation of the external parts. A Cauchy mechanical model such as the hyperelastic model used Fig. 2c cannot have both a very low shear stiffness due to the possible slippage between the fibers and a bending stiffness coming from that of the fibers. The correct modelling of the mechanics of 3D textile reinforcements during their forming requires the use of generalized continuum mechanics.

Two possible continuous approaches to correctly modeling the forming of 3D textile reinforcements are presented in the next two sections. First of all, three-dimensional finite elements are completed by a stiffness related to the curvature which is obtained by the position of the neighbouring elements. Then the local bending stiffness of the fibres is taken into account by a second gradient approach.

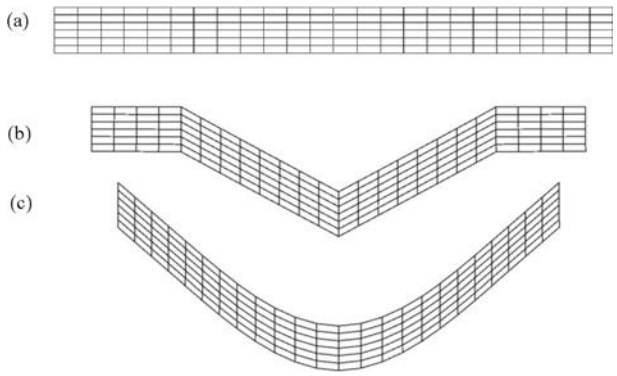

Fig. 3 Basic model **a** hinged bar system: initial state, **b** hinged bar system: deformed shape, **c** beam system

3 Adding Bending Stiffness to 3D Finite Elements

The curvature of a 3D finite element is calculated from the position of the neighboring elements without the need of rotation degree of freedom (Fig. 4a). This approach was initially proposed in the case of rotation free shell elements [35, 36]. Bending nodal loads are computed from these curvatures. They take into account the local fibre bending stiffness.

$$\left(F_{\text{int}}^{\text{bend}}\right)_p = \left(B_1^T M_{l1} + B_2^T M_{l2}\right) A_T \tag{2}$$

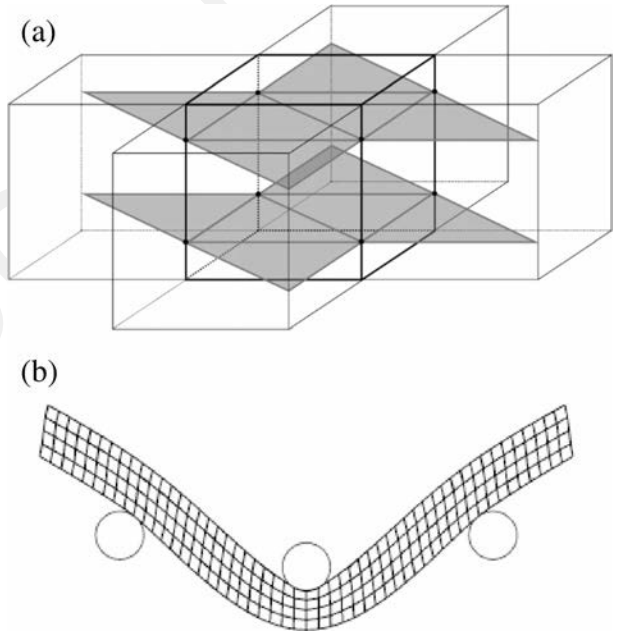

Fig. 4 **a** Computation of the curvature in a hexahedral element, **b** Deformed shape in three point bending test simulation

The bending moments (per length unit) M_{l1}, M_{l2} are function of the curvatures χ_{11}, χ_{22}. The curvature interpolations for a triangle (of surface A_T) inside the element (Fig. 4a) are of the form:

$$\chi_{11} = B_1 u_p \qquad \text{and} \qquad \chi_{22} = B_2 u_p \tag{3}$$

The set of displacements of the adjacent elements of the analyzed triangle constitute u_p and are used to compute the curvatures. The curvature interpolation matrix B_1 and B_2 are detailed in [37].

When these 3D elements with curvature stiffness are used in the case of the three-point bending test presented in section 2 (Fig. 2b for the experiment), the obtained deformed shape is in good agreement with the experiments (Fig. 4b an 2b) [28]. Other simulations based on such enhanced 3D elements can be found in [28, 38].

4 Introducing Fibre Bending Stiffness Using a Second Gradient Approach

Another possible approach to correctly model the bending of textile reinforcements in a 3D framework consists in introducing a second gradient, 3D orthotropic model. To take into account the bending stiffness of fibres, a second gradient potential can be introduced in the 3D orthotropic model of Eq. 1 [25, 39–41]. A term dependent on the gradient of the right Cauchy-green tensor $\mathbf{C}$ is added to the term directly dependent on $\mathbf{C}$:

$$W(\mathbf{C}, \nabla\mathbf{C}) = W_I(\mathbf{C}) + W_{II}(\nabla\mathbf{C}) \tag{4}$$

Here, W_I and W_{II} are respectively, the deformation energy of the Cauchy model (first gradient) and the deformation energy of the second gradient. The latter takes into account the curvature of the continuous medium and thus the local bending of the fibres. Different approaches are possible depending in particular on the internal geometry of the textile reinforcement. The terms of the second gradient generally refer to shear deformations as the fibres are quasi inextensible. The second gradient energy selected in the case of the interlock reinforcement analysed Fig. 2 is as follows:

$$W_{II}(\nabla\mathbf{C}) = W_{II}\left(\nabla I_{cp}, \nabla I_{ct1}, \nabla I_{ct2}\right) = \frac{1}{2} k s_{cp} \left\| \nabla I_{cp} \right\|^2 + \frac{1}{2} k s_{ct1} \left\| \nabla I_{ct1} \right\|^2 + \frac{1}{2} k s_{ct2} \left\| \nabla I_{ct2} \right\|^2 \tag{5}$$

In this second gradient energy, ∇I_{ct1} and ∇I_{ct2} are measurements of the curvatures outside the plane of the two directions of fibres. ∇I_{cp} represents the in-plane curvature of the fibers.

Figure 5 shows the deformed geometry obtained by simulating the three-point bending with a second gradient model. This simulation is in good agreement with the experiment presented Fig. 2b. Second gradient approaches have proved interesting in different cases of composite textile reinforcement forming [41–45].

5 Specific Shell Approach for Textile Reinforcements.

When the thickness of composite textile reinforcements is moderate, shell models can be considered for forming simulation. This is commonly done in draping simulation programs. Currently most of these codes decouple the membrane behavior on the one hand and the

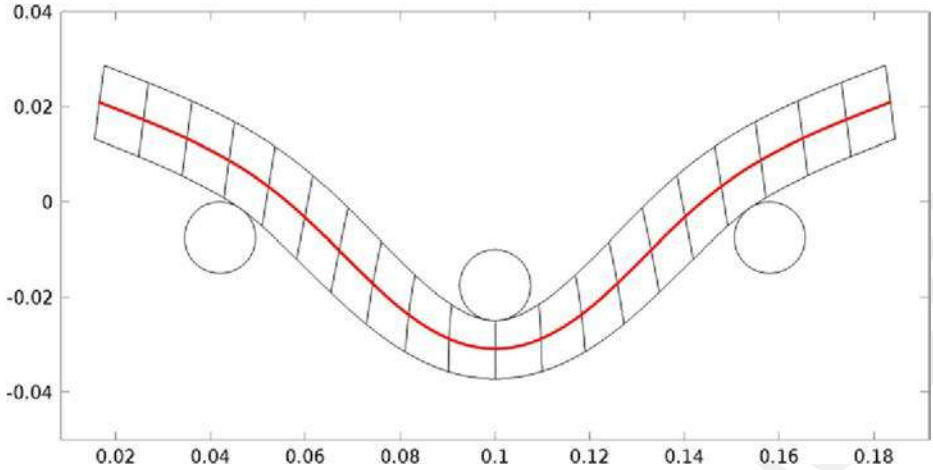

Fig. 5 Simulation of the 3 point bending test based on a second gradient approach [25]

bending behavior on the other hand [37, 46–52]. This decoupling reflects the fact that conventional shell approaches are not satisfactory for fibrous media. If this decoupling is effective for the deformation of the average surface of the fibrous reinforcement, in particular for the simulation of wrinkles [53–55], it does not give the distribution of deformations and stresses for the points in the thickness what a shell model is supposed to do. The bending behaviour of a textile reinforcement is strongly conditioned by the possible slip between the fibres and is not correctly modelled by standard Kirchhoff and Mindlin theories. In particular, bending stiffness cannot be deduced from membrane stiffness and thickness as is the case for classical plate theories.

The bending deformation energy of textile reinforcements is determined by the bending moment that can be assumed to depend on the curvature. The relationship $M(\chi)$ (bending moment-curvature) can be determined by experimental methods [56–58]. The material normals initially perpendicular to the mean surface remain perpendicular to the mean surface after deformation in Kirchhoff's theory. Figs. 2 and 6 show that the material normals do not remain perpendicular to the deformed average surface and that the textile reinforcements do not follow Kirchhoff's theory at all. The curvature is the derivative of the rotation of the normal in Mindlin's theory. It can be seen that this is not the case in Fig. 6a between sections 1 and 3. Generally speaking, textile reinforcements do not verify Mindlin's theory and it is not possible to simulate the flexion of a textile reinforcement using Mindlin's shell finite elements.

The bending of the textile reinforcements is based on a specific physics. The two particular points are the quasi-inextensibility of the fibres on the one hand and the possible slippage between the fibres on the other. A shell finite element for composite textile reinforcements has been proposed by Liang et al. [29]. This element is based on Ahmad's approach [59]. It consists of parallel fibres (Fig. 6c). The internal virtual work of the element is equal to the sum of the virtual work of tension and bending of each fiber.

$$\delta W^e_{\text{int}} = \sum_{f=1}^{n} \int_{L^f} T^{11f}\, \delta {\varepsilon_{11}}^f\, dL + \sum_{f=1}^{n} \int_{L^f} M^{33f}\, \delta {\chi_{33}}^f\, dL \tag{6}$$

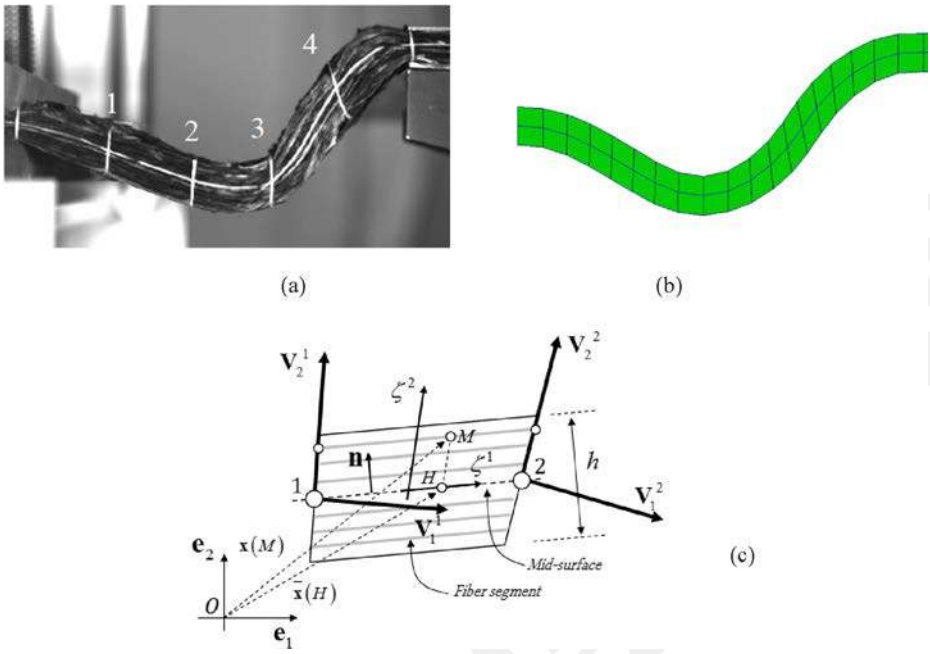

Fig. 6 Bending test on a multilayer reinforcement: **a** Experiment, **b** Simulation, **c** Ahmad shell finite element

The tensile stress in a fibre *f* is noted T^{11} and the bending moment M^{33}. $\delta\varepsilon_{11}$ is the virtual tensile strain. $\delta\chi_{33}$ is the virtual curvature. The curvatures and the axial strains in the fibres are calculated using adjacent elements.

The results obtained with this specific woven shell element are in good agreement with experiment. The normal rotations are relevant (Figs. 6 and 7). Fig. 7 shows simulation of the three-point bending test of the interlock reinforcement studied in Section 2.

A small number of degrees of freedom (20 dof in Fig. 6) is sufficient to obtain accurate results. The bending stiffness is strongly related to the friction between the fibres and the influence of this friction can be taken into account in the bending stiffness of each fibre. Further simulations and comparisons with experiments are presented in [29]. The present approach should be extended to 3D cases.

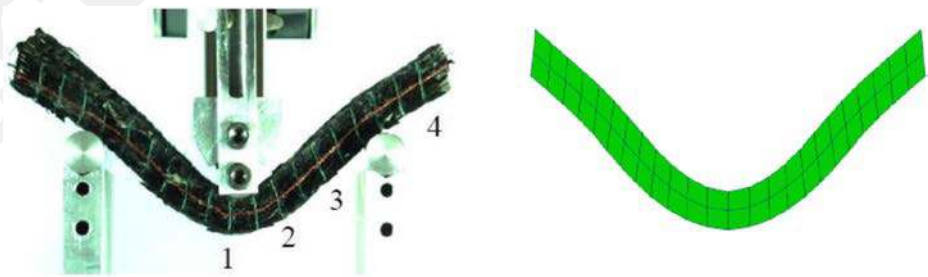

Fig. 7 Three points bending tests on an interlock reinforcement: Left: experiment, right: simulation .using the specific shell element

6 Conclusion

The deformation of textile reinforcements is based on a specific physics. Mainly, the quasi-inextensibility of the fibres on the one hand and the possible slippage between the fibers on the other. Bending of textile reinforcements is not adequately modelized by standard bending theories. It has been demonstrated that the standard continuous Cauchy models cannot correctly describe the deformation of the textile reinforcements. Such a Cauchy model cannot take into account the possible slip between the fibres at the same time as the local bending stiffness of the fibres. It is therefore necessary to develop generalized continuum mechanics models that are simple and effective enough for the simulation of textile reinforcement forming. A theory for the flexion of the fibrous reinforcements is also necessary.

One can ask what happens when the polymer is present. The phenomena highlighted and studied in this article concern fibrous reinforcements. They are based mainly on two specificities: the inextensibility of the fibres and the possible relative slip of the fibres during deformation. When the matrix is present it can be hardened (composite material) or not (prepreg). In the case of prepregs, the two previous points (inextensibility and slippage between fibres) remain true because the matrix is not hardened. When the matrix is hardened (composite material) the sliding between the fibres is no longer possible (this is the role of the matrix). Consequently, in the first analysis it can be said that the behaviours highlighted in the present work for textile reinforcements (second gradient) do not extend to composite materials (with cured resin).

References

1. Weimer, C.: The future composite materials challenge in aeronautics. In: ECCM 17 conference, Munich (2016)
2. Meola, C., Boccardi, S.: Composite materials in the aeronautical industry. Infrared Thermography to Composites, Woodhead. 1–24 (2017)
3. Friedrich, K., & Almajid, A. A. (2013). Manufacturing aspects of advanced polymer composites for automotive applications. Applied Composite Materials, Applied Composite Materials, 20(2), 107-128
4. Smith, C.S.: Design of marine structures in composite materials. London: Elsevier applied. Science. (1990)
5. Bowen, D.H.: Applications of composites: an overview. In: Kelly, A. (ed.) Concise Encyclopedia of Composite Materials, pp. 7–15. Pergamon Press, Oxford (1989)
6. Douthe, C., Baverel, O., Caron, J.F.: Form-finding of a grid Shell in composite materials. Journal of the International Association For Shell And Spatial Structures. **47**, 53 (2006)
7. Mouritz, A.P., Bannister, M.K., Falzon, P.J., Leong, K.H.: Review of applications for advanced three-dimensional fibre textile composites. Composites Part A. **30**, 1445–1461 (1999)
8. Tong, L., Mouritz, A.P., Bannister, M.K.: 3D Fibre Reinforced Polymer Composites. Elsevier Science (2002)
9. Lomov, S.V., Gusakov, A., Huysmans, G., Prodromou, A.G., Verpoest, I.: Textile geometry preprocessor for meso-mechanical models of woven composites. Compos. Sci. Technol. **60**(11), 2083–2095 (2000)
10. Bigaud, D., Dreano, L., Hamelin, P.: Models of interactions between process, microstructure and mechanical properties of composite materials–a study of the interlock layer-to-layer braiding technique. Compos. Struct. **67**(1), 99–114 (2005)
11. Dufour, C., Wang, P., Boussu, F., Soulat, D.: Experimental investigation about stamping behaviour of 3D warp interlock composite preforms. Appl. Compos. Mater. **21**(5), 725–738 (2014)
12. Lapeyronnie, P., Le Grognec, P., Binetruy, C., Boussu, F.: Homogenization of the elastic behavior of a layer-to-layer angle-interlock composite. Compos. Struct. **93**(11), 2795–2807 (2011)
13. Wendling, A., Hivet, G., Vidal-Sallé, E., Boisse, P.: Consistent geometrical modelling of interlock fabrics. Finite Elem. Anal. Des. **90**, 93–105 (2014)
14. Wendling, A., Daniel, J.L., Hivet, G., Vidal-Sallé, E., Boisse, P.: Meshing preprocessor for the Mesoscopic 3D finite element simulation of 2D and interlock fabric deformation. Appl. Compos. Mater. **22**(6), 869–886 (2015)

15. Chen, X. (ed.): Advances in 3D Textiles. Elsevier (2015)
16. Boussu, F., Cristian, I., Nauman, S.: General definition of 3D warp interlock fabric architecture. Compos. Part B. **81**, 171–188 (2015)
17. Gong, X., Chen, X., Zhou, Y.: Advanced weaving technologies for high-performance fabrics. In high-performance. Apparel. 75–112 (2017)
18. De Luycker, E., Morestin, F., Boisse, P., Marsal, D.: Simulation of 3D interlock composite preforming. Compos. Struct. **88**(4), 615–623 (2009)
19. Creech, G., Pickett, A.K.: Meso-modelling of non-crimp fabric composites for coupled drape and failure analysis. J. Mater. Sci. **41**(20), 6725–6736 (2006)
20. Lomov, S.V., Ivanov, D.S., Verpoest, I., Zako, M., Kurashiki, T., Nakai, H., Hirosawa, S.: Meso-FE modelling of textile composites: road map, data flow and algorithms. Compos. Sci. Technol. **67**(9), 1870–1891 (2007)
21. Bel, S., Hamila, N., Boisse, P., Dumont, F.: Finite element model for NCF composite reinforcement preforming: importance of inter-ply sliding. Compos. A: Appl. Sci. Manuf. **43**(12), 2269–2277 (2012)
22. Gatouillat, S., Bareggi, A., Vidal-Sallé, E., Boisse, P.: Meso modelling for composite preform shaping–simulation of the loss of cohesion of the woven fibre network. Compos. A: Appl. Sci. Manuf. **54**, 135–144 (2013)
23. Forest, S.: Micromorphic approach for gradient elasticity, viscoplasticity, and damage. J. Eng. Mech. **135**(3), 117–131 (2009)
24. Maugin, G.A.: Generalized continuum mechanics: what do we mean by that? Mechanics of Generalized Continua. 3–13 (2010)
25. Madeo, A., Ferretti, M., Dell'Isola, F., Boisse, P.: Thick fibrous composite reinforcements behave as special second-gradient materials: three-point bending of 3D interlocks. Z. Angew. Math. Phys. **66**(4), 2041–2060 (2015)
26. d'Agostino, M.V., Giorgio, I., Greco, L., Madeo, A., Boisse, P.: Continuum and discrete models for structures including (quasi-) inextensible elasticae with a view to the design and modeling of composite reinforcements. Int. J. Solids Struct. **59**, 1–17 (2015)
27. Boisse, P., Hamila, N., Madeo, A.: The difficulties in modeling the mechanical behavior of textile composite reinforcements with standard continuum mechanics of Cauchy. Some possible remedies. International Journal of Solids and Structures. On Line. (2018). https://doi.org/10.1016/j.ijsolstr.2016.12.019
28. Mathieu, S., Hamila, N., Bouillon, F., Boisse, P.: Enhanced modeling of 3D composite preform deformations taking into account local fiber bending stiffness. Compos. Sci. Technol. **117**, 322–333 (2015)
29. Liang, B., Colmars, J., Boisse, P.: A shell formulation for fibrous reinforcement forming simulations. Compos. A: Appl. Sci. Manuf. **100**, 81–96 (2017)
30. Boisse, P., Colmars, J., Hamila, N., Naouar, N., Steer, Q.: Bending and wrinkling of composite fiber preforms and prepregs. A review and new developments in the draping simulations. Composites Part B. **141**, 234–249 (2018)
31. Naouar N., analyse mésoscopique par éléments finis de la déformation de renforts fibreux 2d et 3d à partir de microtomographies X, Ph.D. thesis, University of Lyon, 2015
32. Carvelli, V., Pazmino, J., Lomov, S.V., Verpoest, I.: Deformability of a non-crimp 3D orthogonal weave E-glass composite reinforcement. Compos. Sci. Technol. **73**, 9–18 (2012)
33. Charmetant, A., Orliac, J.G., Vidal-Sallé, E., Boisse, P.: Hyperelastic model for large deformation analyses of 3D interlock composite preforms. Compos. Sci. Technol. **72**(12), 1352–1360 (2012)
34. Boehler, J.P.: Lois de comportement anisotrope des milieux continus. J. Méc. **17**, 153–170 (1978)
35. Onate, E., Zarate, F.: Rotation-free triangular plate and shell elements. Int. J. Numer. Methods Eng. **47**, 557–603 (2000)
36. Brunet, M., Sabourin, F.: Analysis of a rotation-free 4-node shell element. Int. J. Numer. Methods Eng. **66**, 1483–1510 (2006)
37. Hamila, N., Boisse, P., Sabourin, F., Brunet, M.: A semi-discrete shell finite element for textile composite reinforcement forming simulation. Int. J. Numer. Methods Eng. **79**(12), 1443–1466 (2009)
38. Mathieu, S., Hamila, N., Dupé, F., Descamps, C., Boisse, P.: Stability of 3D textile composite reinforcement simulations: solutions to spurious transverse modes. Appl. Compos. Mater. **23**(4), 739–760 (2016)
39. Spencer, A.J.M., Soldatos, K.P.: Finite deformations of fibre-reinforced elastic solids with fibre bending stiffness. International Journal of Non-Linear Mechanics. **42**(2), 355–368 (2007)
40. dell' Isola, F., Steigmann, D.: A two-dimensional gradient-elasticity theory for woven fabrics. J. Elast. **118**(1), 113–125 (2015)
41. Ferretti, M., Madeo, A., dell'Isola, F., Boisse, P.: Modeling the onset of shear boundary layers in fibrous composite reinforcements by second-gradient theory. Z. Angew. Math. Phys. **65**, 587–612 (2014)
42. Madeo, A., Barbagallo, G., d'Agostino, M.V., Boisse, P.: Continuum and discrete models for unbalanced woven fabrics. Int. J. Solids Struct. **94**, 263–284 (2016)

43. Barbagallo, G., Madeo, A., Morestin, F., Boisse, P.: Modelling the deep drawing of a 3D woven fabric with a second gradient model. Mathematics and Mechanics of Solids. **22**(11), 2165–2179 (2017)
44. Seppecher, P., Alibert, J. J., & Isola, F. D. (2011). Linear elastic trusses leading to continua with exotic mechanical interactions. In J. Phys. Conf. Ser. (Vol. 319, No. 1, p. 012018). IOP Publishing
45. Giorgio, I., Della Corte, A., Dell'Isola, F., Steigmann, D.J.: Buckling modes in pantographic lattices. Comptes rendus Mecanique. **344**(7), 487–501 (2016)
46. Hübner, M., Rocher, J.E., Allaoui, S., Hivet, G., Gereke, T., Cherif, C.: Simulation-based investigations on the drape behavior of 3D woven fabrics made of commingled yarns. Int. J. Mater. Form. **9**(5), 591–599 (2016)
47. Döbrich, O., Gereke, T., Diestel, O., Krzywinski, S., Cherif, C.: Decoupling the bending behavior and the membrane properties of finite shell elements for a correct description of the mechanical behavior of textiles with a laminate formulation. J. Ind. Text. **44**(1), 70–84 (2014)
48. Hamila, N., Boisse, P.: A meso–macro three node finite element for draping of textile composite preforms. Appl. Compos. Mater. **14**(4), 235–250 (2007)
49. Gereke, T., Döbrich, O., Hübner, M., Cherif, C.: Experimental and computational composite textile reinforcement forming: a review. Compos. A: Appl. Sci. Manuf. **46**, 1–10 (2013)
50. Haanappel, S.P., Ten Thije, R.H.W., Sachs, U., Rietman, B., Akkerman, R.: Formability analyses of uni-directional and textile reinforced thermoplastics. Composites Part A. **56**, 80–92 (2014)
51. Zouari, B., Daniel, J.L., Boisse, P.: A woven reinforcement forming simulation method. Influence of the shear stiffness. Comput. Struct. **84**(5–6), 351–363 (2006)
52. Dörr, D., Schirmaier, F.J., Henning, F., Kärger, L.: A viscoelastic approach for modeling bending behavior in finite element forming simulation of continuously fiber reinforced composites. Compos. A: Appl. Sci. Manuf. **94**, 113–123 (2017)
53. Boisse, P., Hamila, N., Vidal-Sallé, E., Dumont, F.: Simulation of wrinkling during textile composite reinforcement forming. Influence of tensile, in-plane shear and bending stiffnesses. Compos. Sci. Technol. **71**(5), 683–692 (2011)
54. Skordos, A.A., Aceves, C.M., Sutcliffe, M.P.F.: A simplified rate dependent model of forming and wrinkling of pre-impregnated woven composites. Compos. Part A. **38**, 1318–1330 (2007)
55. Sjölander, J., Hallander, P., Åkermo, M.: Forming induced wrinkling of composite laminates: a numerical study on wrinkling mechanisms. Compos. A: Appl. Sci. Manuf. **81**, 41–51 (2016)
56. Peirce, F.T.: The geometry of cloth structure. J Textil Inst Trans. **28**(3), T45–T96 (1937)
57. De Bilbao, E., Soulat, D., Hivet, G., Gasser, A.: Experimental study of bending behavior of reinforcements. Exp. Mech. **50**(3), 333–351 (2010)
58. Liang, B., Hamila, N., Peillon, M., Boisse, P.: Analysis of thermoplastic prepreg bending stiffness during manufacturing and of its influence on wrinkling simulations. Compos Part A: Appl Sci Manuf. **67**, 111–122 (2014)
59. Ahmad, S., Irons, B.M., Zienkiewicz, O.C.: Analysis of thick and thin shell structures by curved finite elements. Int. J. Numer. Methods Eng. **2**(3), 419–451 (1970)